Supplement of Atmos. Chem. Phys., 21, 14649–14669, 2021
https://doi.org/10.5194/acp-21-14649-2021-supplement

Atmospheric Chemistry and Physics
Open Access
EGU

Supplement of

Evolution of OH reactivity in NO-free volatile organic compound photooxidation investigated by the fully explicit GECKO-A model

Zhe Peng et al.

Correspondence to: Zhe Peng (zhe.peng@colorado.edu) and Jose L. Jimenez (jose.jimenez@colorado.edu)

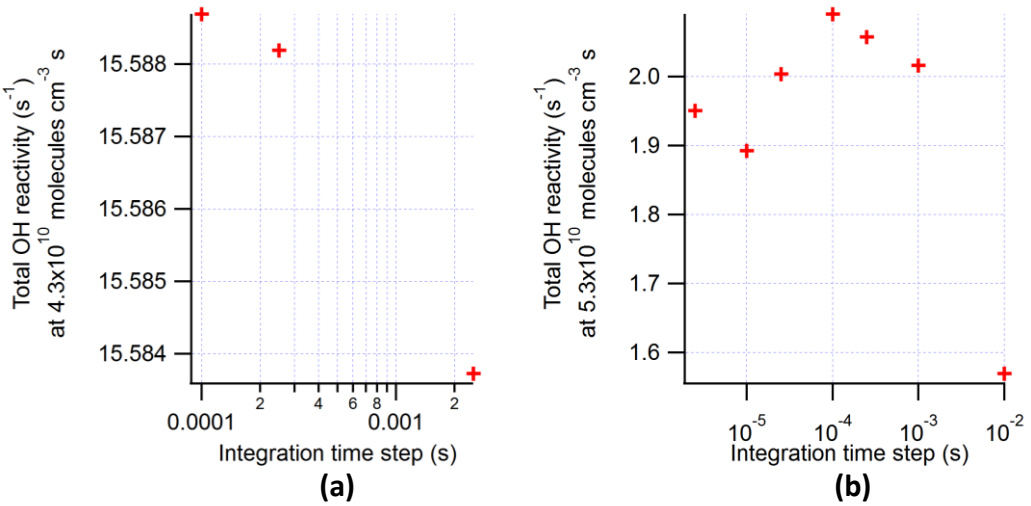

Figure S1. Total OH reactivity (OHR) of organics at OH exposure of (a) 4.3×10^{10} ad (b) 5.3×10^{10} molecules cm^{-3} s as a function of integration timestep in the test simulations for the (a) m-xylene and (b) isoprene oxidation flow reactor (OFR) cases at relative humidity of 70%, high lamp setting, and initial OHR of 10 s^{-1}. Note that the mechanisms in these test simulations are similar but not exactly the same as in the corresponding model cases shown in Table 1.

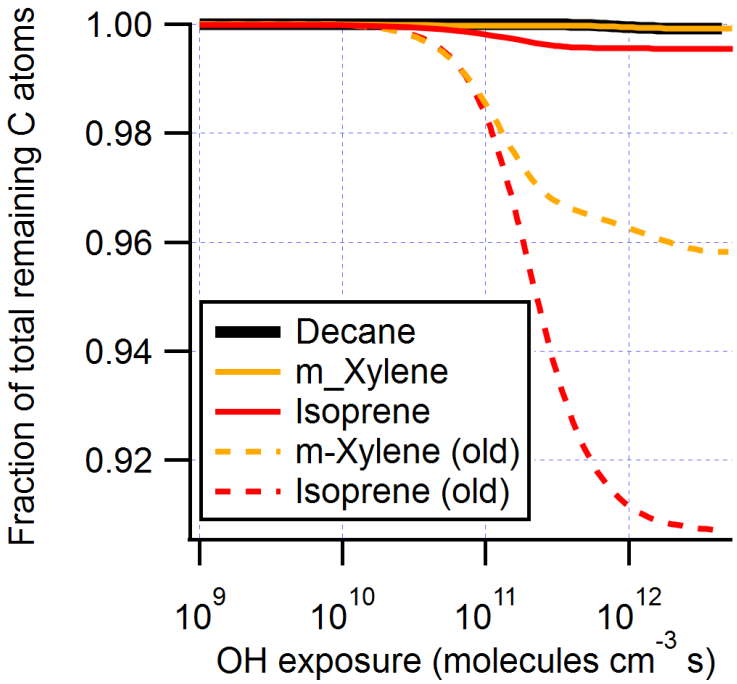

Figure S2. Fractions of total remaining C atoms as a function of OH exposure in the ambient cases with constant sunlight of the photooxidations of decane, m-xylene, and isoprene. Also shown for comparison are the simulations for m-xylene and isoprene with the old mechanisms whose problem of non-conservation of C atoms in some reactions has not been fixed.

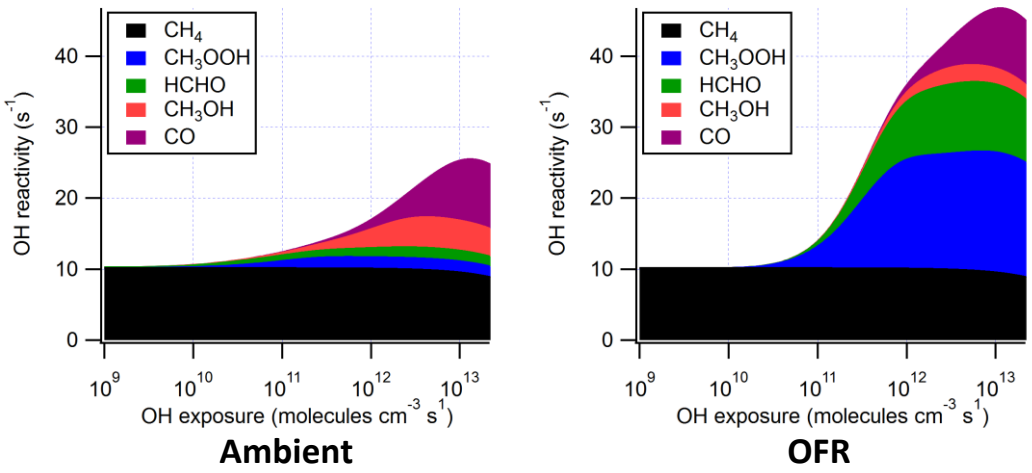

Figure S3. OH reactivity (OHR) of the organics as a function of OH exposure in the ambient case with constant sunlight; and in the OFR case at relative humidity of 70% and high lamp setting, both with initial OHR of 10 s^{-1} of methane photooxidation.

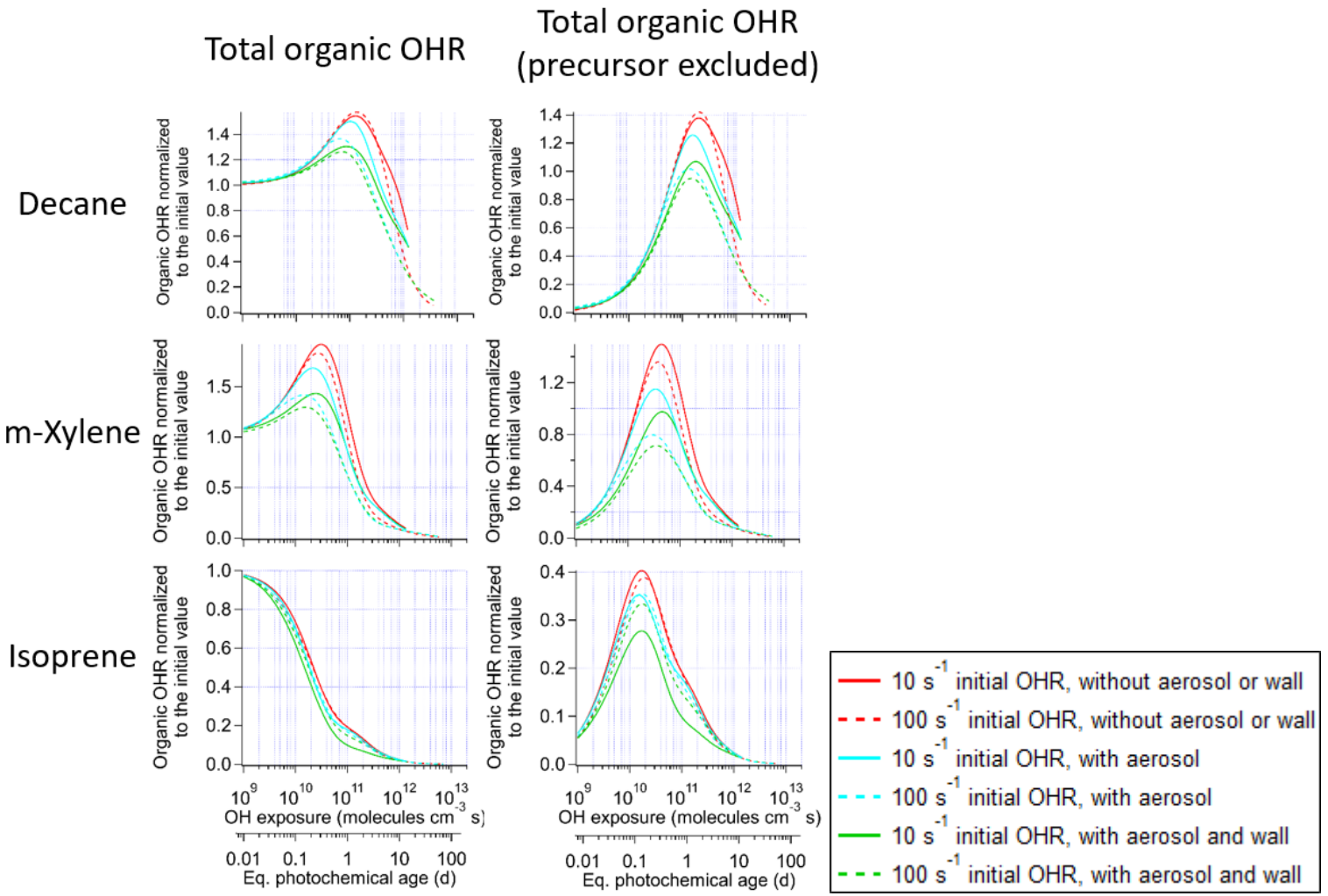

Figure S4. Same format as Fig. 1, but for the chamber cases without aerosol or wall, with aerosol (no wall), and with aerosol and wall for decane, m-xylene, and isoprene photooxidation.

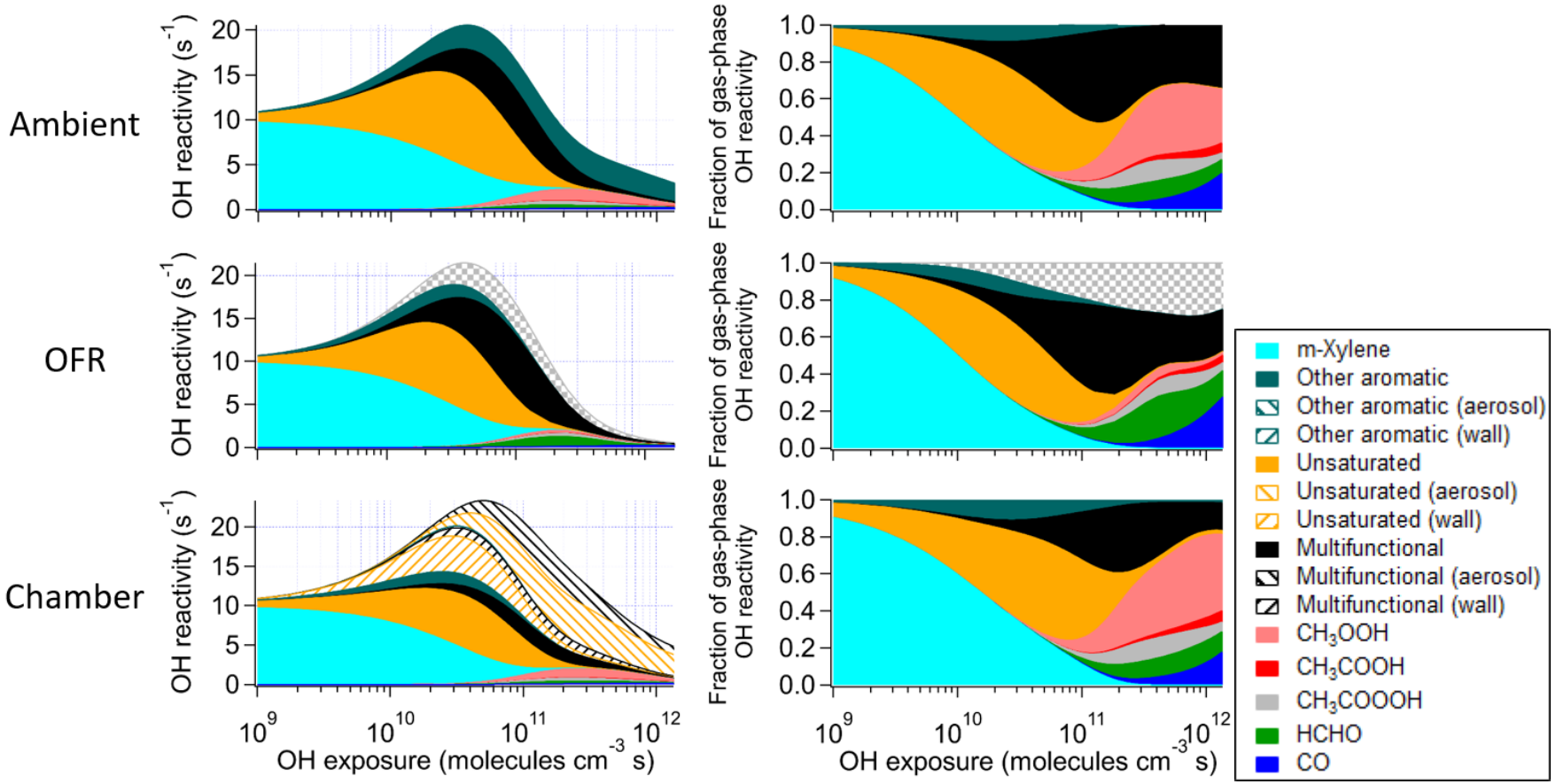

Figure S5. Same format as Fig. 4, but for m-xylene photooxidation.

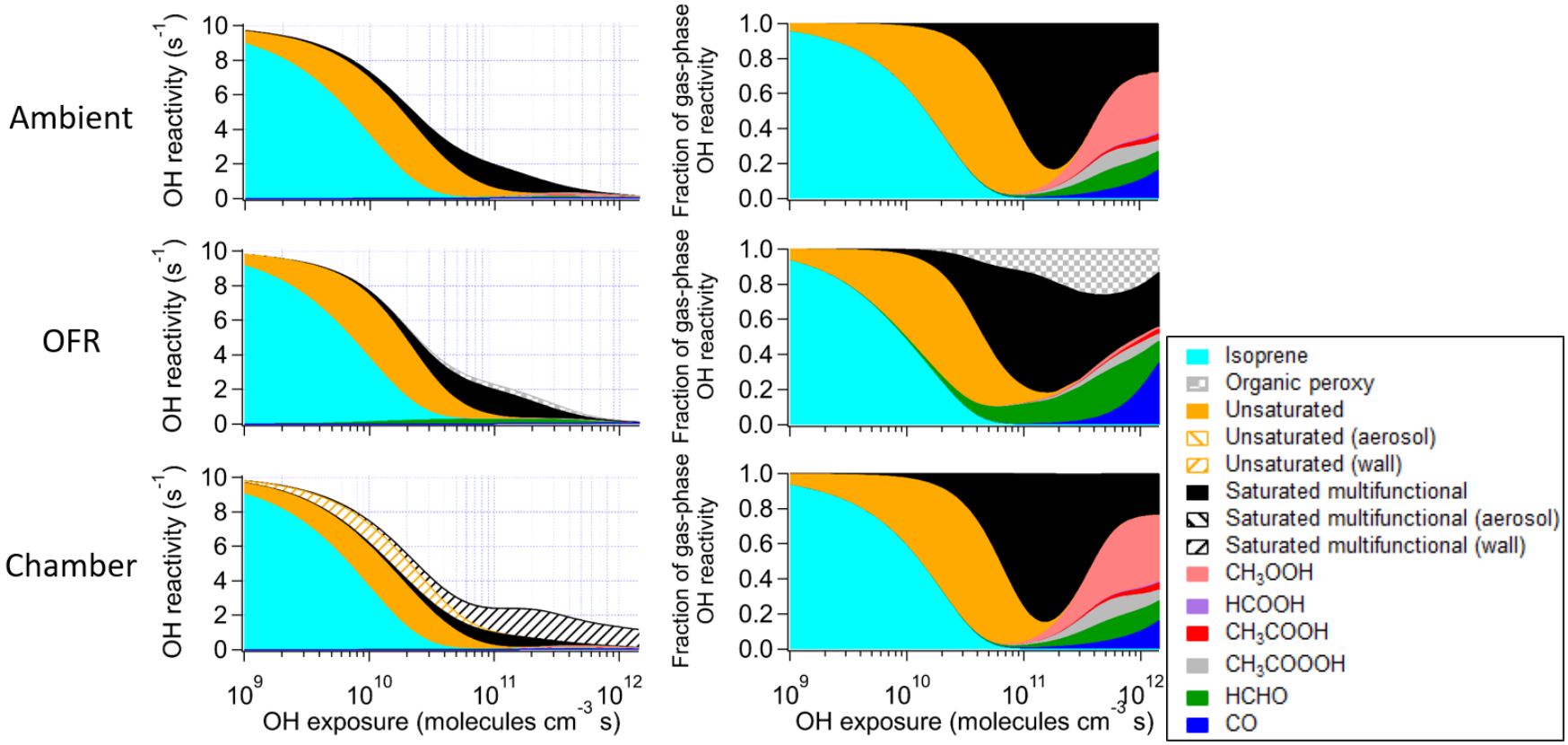

Figure S6. Same format as Fig. 4, but for isoprene photooxidation.

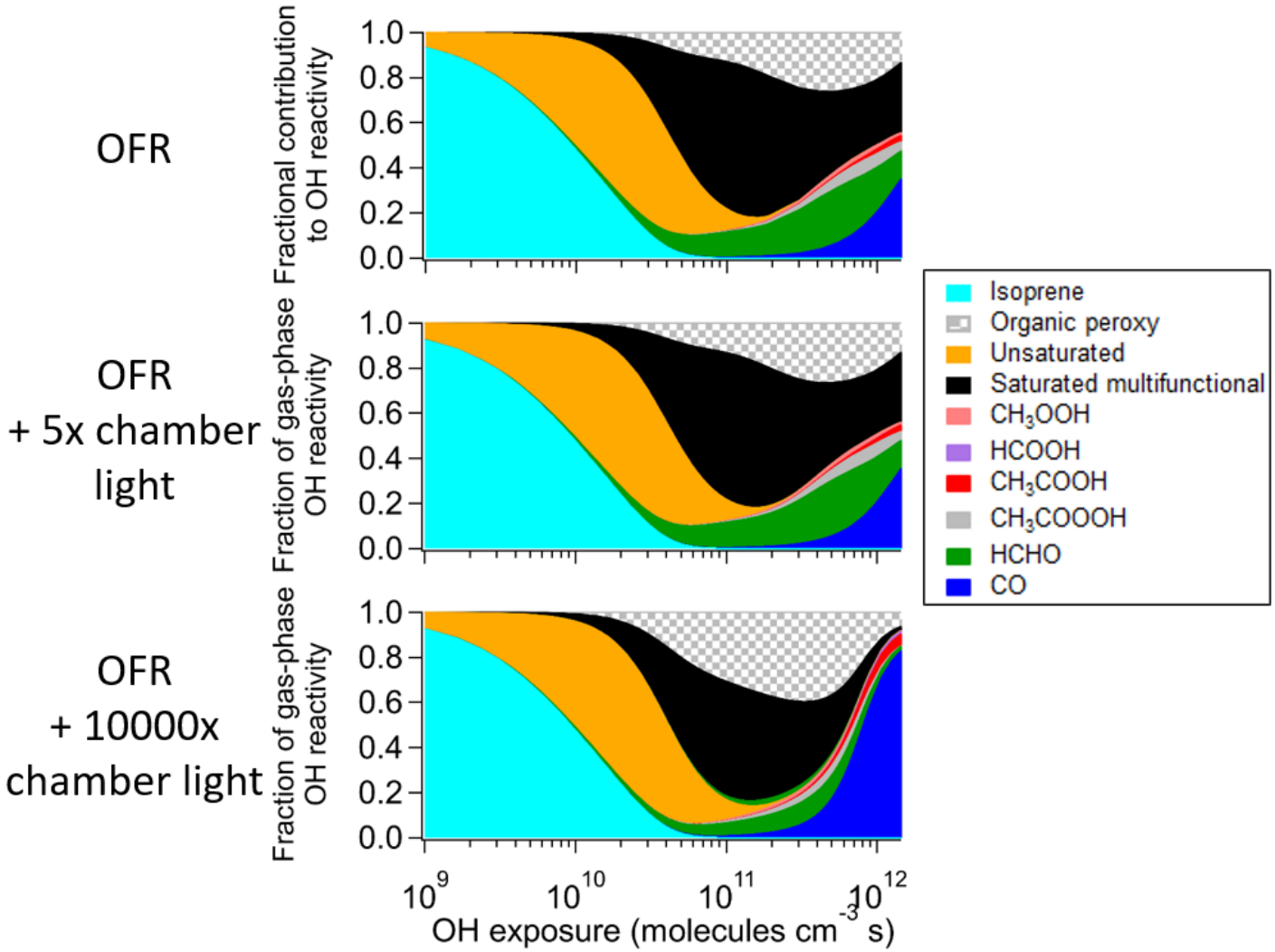

Figure S7. Fractional contributions of the main species and types of species to the organic OHR as a function of OH exposure in the standard OFR case of isoprene photooxidation with relative humidity of 30%, medium UV lamp setting, and two sensitivity cases based on this OFR case, with additional UV irradiation corresponding to 5 and 10000 times the UV source of the University of Colorado Environmental Chamber Facility, respectively. The types of species shown in this figure exclude the C1 and C2 species listed separately.

Scheme S1. Mechanism of xylenol photooxidation in the absence of NO, derived from MCM v3.2 (Jenkin et al., 2003; Bloss et al., 2005). Panel a): All meta-xylene reaction channels; Panel b): Xylenol reaction channels, expanded. Numbers refer to branching ratios. Green text indicates products from MCM v3.2; blue text indicates products generated by GECKO-A and added in this study; blue-and-green indicates products provided by both MCM3.2 and GECKO-A. Species whose products persist anomalously under zero-NO conditions are indicated with green dashed borders. Short dotted arrows indicate chemistry continuing according to standard SARs. Dashed arrows indicate photolysis pathways (which are usually minor). For illustration, we extend the dominant (HO_2 and higher branching ratio OH) oxidation pathway of one of the most prevalent RO_2 products (2T800J: panel b, lower center to upper right). Its main pathway from initial OH oxidation (lower right, 2nd row up) is also extended to show an example of typical ring-breaking chemistry. Net OH rate constants for MXYLOOH, MXY1OOH, MXYCATECH, and MXYLAL are $1.77x10^{-11}$, $3.26x10^{-11}$, $1.56x10^{-10}$ and $8.6x10^{-13}$ cm3 $molecule^{-1}$ s^{-1} respectively. (The MXYLOOH OH rate includes MXYLAL production). Figure adapted from MCM website, http://mcm.leeds.ac.uk/MCMv3.3.1, accessed July 3, 2020.

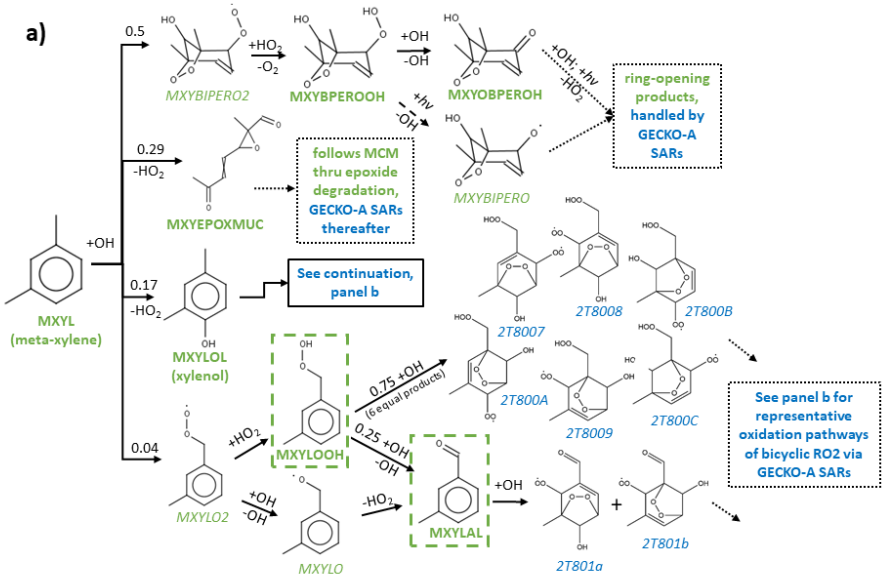

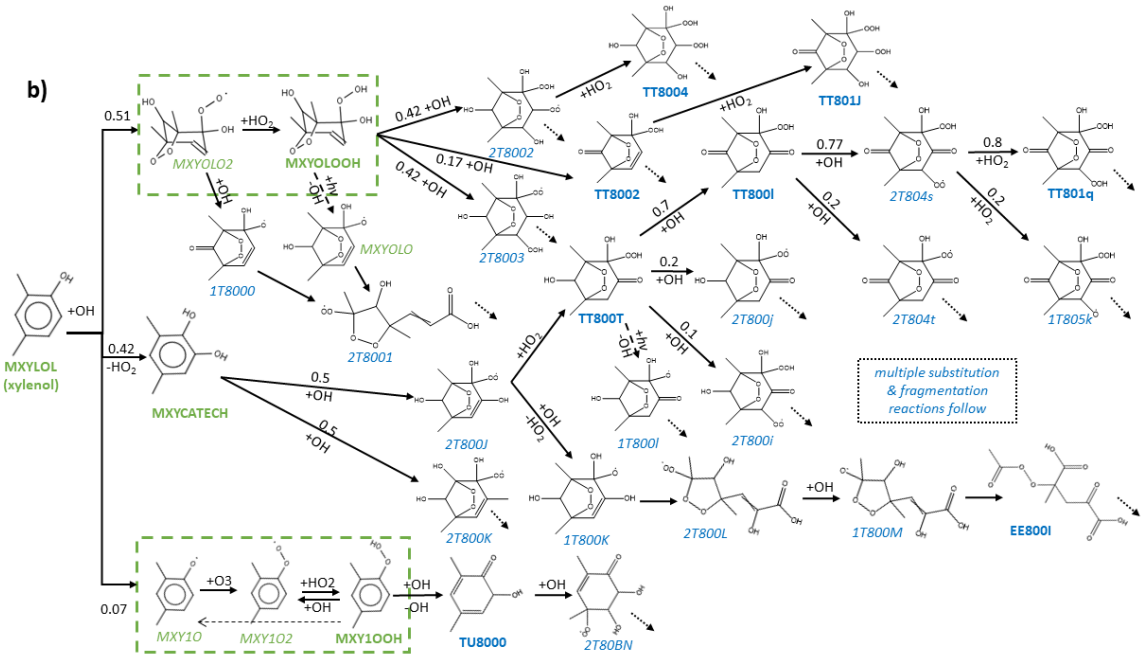
b)
MXYLOL (xylenol)
+OH
0.51
0.42
-HO2
0.07
MXYOLO2
MXYOLOOH
+HO2
MXYCATECH
MXYOLO
1T8000
2T8001
2T8002
2T8003
TT8004
TT8002
TT800T
TT800I
TT801J
2T804s
TT801q
2T800j
2T804t
1T805k
2T800J
1T800I
2T800i
2T800K
1T800K
2T800L
1T800M
EE800I
multiple substitution & fragmentation reactions follow
MXY1O
MXY1O2
MXY1OOH
+O3
+HO2
TU8000
2T80BN
0.42 +OH
0.17 +OH
0.7 +OH
0.2 +OH
0.77 +OH
0.8 +HO2
0.5 +OH
0.1 +OH
-OH +hν
-HO2
+HO2
+OH

Scheme S2. Mechanism of methane photooxidation. Numbers refer to branching ratios.

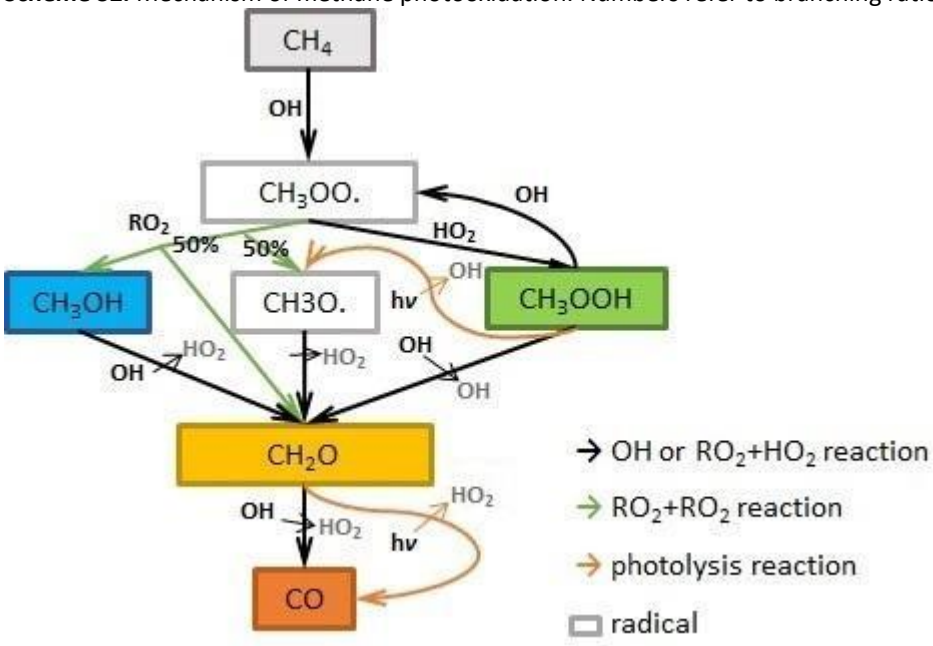

Table S1. Extension of reference absorption cross-sections (σ) and branching ratios (ϕ) of organic photolysis to 185 nm and 254 nm

Species, channel	σ_{185nm}	Φ_{185nm} (if ≠ 1)
CH_2O	3.64×10^{-18} Cooper (1996) 184 nm	
$\longrightarrow H_2 + CO$		0.44 Formula extrapolation, Röth (2015)
$\longrightarrow HCO + H$		0.56 Formula extrapolation, Röth (2015)
CH_3OOH	9.0×10^{-19} rough extrapolation from 210-280nm data[a]	
$CH_2(OH)OOH$	9.0×10^{-19} estimate after CH_3OOH	
CH_3CHO	7.84×10^{-20} [a]	
CHOCHO	4.80×10^{-19} Zhu (1996) at 193nm	
$\longrightarrow H_2 + 2\ CO$		0.81 data extrapolation[b] (225nm)
$\longrightarrow 2\ CHO$		0.16 data extrapolation[b] (225nm)
$\longrightarrow CH_4+CO$		0.03 data extrapolation[b] (225nm)
$CH_2(OH)CHO$	3.85×10^{-18} Karandunandan (2007) at 184.9nm	
CH(O)C(O)OH	4.0×10^{-19} rough extrapolation from Back & Yamamoto (1985) (200nm)	
$\longrightarrow HCHO + CO_2$		0.84
$\longrightarrow HCO + 2\ CO$		0.16
C(O)(OH)C(O)OH	1.0×10^{-18} estimate after CH(O)C(O)OH and $CH_3C(O)C(O)OH$	
$\longrightarrow HC(O)OH + CO_2$		0.72 Yamamoto (1985) (255-309 nm)
$\longrightarrow HC(O)OH + CO_2$		0.27 Yamamoto (1985) (255-309 nm)
CH_3CH_2CHO	1.43×10^{-17} Lucazeau & Sandorfy (1970) (184.8 nm)	
CH_3COCH_3	2.96×10^{-18} Gierczak (2003) (184.9 nm, 242 K) *[note: 296K value is 3.01×10^{-18}]*	
CH_3COCHO	3.71×10^{-18} data extrapolation[b] (200-215 nm)	
$\longrightarrow CH_3C(.)O + CHO.$		0.90 Raber (1995) (220-320 nm)
$\longrightarrow CH_3CHO + CO$		0.05 Raber (1995) (220-320 nm)
$\longrightarrow CH_4 + 2\ CO$		0.05 Raber (1995) (220-320 nm)
CH_3COCH_2OH	5.40×10^{-18} Dillon (2006) (184.9 nm)	
		0.6 Orlando (1999) (236-340 nm)
$CH_3C(O)C(O)OH$	1.0×10^{-17} rough extrapolation from JPL 10-6 (252-280 nm)	
		0.37 Moortgat (1999) (251-400 nm)

Species, channel	σ_{254nm}	Φ_{254nm}
CHOCHO	1.60×10^{-20} Volkamer (2005) at 254nm	
$\longrightarrow H_2 + 2\ CO$		0.54 data interpolation[b]
$\longrightarrow 2\ CHO$		0.16 data interpolation[b]
$\longrightarrow CH_4+CO$		0.32 data interpolation[b]
C(O)(OH)C(O)OH	6.55×10^{-20} extrapolation from Yamamoto (1985) (255-260 nm)	
$\longrightarrow HC(O)OH + CO_2$		0.72 Yamamoto (1985) (255-309 nm)
$\longrightarrow CO_2 + CO + H_2O$		0.27 Yamamoto (1985) (255 -309 nm)

[a] Data from online spectral atlas: Keller-Rudek, H., Moortgat, G. K., Sander, R., and Sörensen, R., The MPI-Mainz UV/VIS spectral atlas of gaseous molecules of atmospheric interest, Earth Syst. Sci. Data, 5, 365–373, (2013)
[b] Data from JPL 10-6 (Sander et al, 2011)

Table S2. Major contributors (>0.1 s-1 or the first 20) to the OH reactivity at 1x1010, 1x1011, and 1x1012 molecules cm-3 s in the ambient case with constant UV of the photooxidation of decane, m-xylene, and isoprene. Also shown is the percentage of OH reactivity accounted for by the species reported in this table. Positional isomers with identical rate constant with OH are lumped into a single species. See Scheme S1 for the structures of the special names for m-xylene oxidation in this table. The "C1-O-C1" string in the names represents an epoxide structure. The isoprene case has no species contributing >0.1 s-1 to the total OH reactivity at 1x1012 molecules cm-3 s, and is thus not shown for this OH exposure.

Precursor	OH exposure (molecules cm^{-3} s)	Species name	OH reactivity (s^{-1})	Percentage of OH reactivity accounted for
decane	$1x10^{10}$	decane	8.97	>99
		decyl hydroperoxide	1.95	
		dihydroperoxy decane	0.12	
	$1x10^{11}$	decyl hydroperoxide	5.06	94
		decane	3.35	
		dihydroperoxy decane	2.17	
		hydroperoxy decanone	1.65	
		decanone	1.18	
		dioxodecyl hydroperoxide	0.36	
		hydroxydecyl hydroperoxide	0.27	
		dioxodecane	0.14	
		hydroxydecyl dihydroperoxide	0.13	
		hydroperoxyhydroxydecanone	0.11	
	$1x10^{12}$	CH3OOH	0.88	53
		HCHO	0.63	
		CH_3CH_2OOH	0.36	

		$CH_3C(O)OOH$	0.31	
		CH_3CHO	0.31	
		$HOOCH_2C(O)OOH$	0.23	
		$CH_3C(O)CH_2CH_2OOH$	0.23	
		$CH_3C(O)CH_2OOH$	0.21	
		$HOOCH_2CH_2OOH$	0.20	
		$HOOCH_2COOH$	0.20	
		CO	0.19	
		$HOOCH_2CHO$	0.17	
		$CH_3C(O)CH_2CHO$	0.17	
		$HOOCH_2CH_2C(O)OOH$	0.13	
		$HOOCH_2CH_2COOH$	0.12	
		$CH_3CH_2C(O)CH_2CH_2OOH$	0.11	
m-xylene	$1x10^{10}$	m-xylene	7.92	96
		MXYBPEROOH	2.99	
		MXYEPOXMUC	1.41	
		MXYOBPEROH	1.13	
		m-xylenol	0.90	
		$CH_3C(O)CH(OOH)CH(OH)C1H\text{-}O\text{-}C1(CH_3)CHO$	0.34	
		dimethyl catechol	0.22	
		MXYOLOOH	0.17	

	$1x10^{11}$	methylglyoxal	1.04	69
		m-xylene	0.96	
		CH_3OOH	0.91	
		MXYOBPEROH	0.81	
		MXYBPEROOH	0.59	
		$CH_3C(OOH)(CHO)_2$	0.45	
		$CH_3C1(CHO)$-O-C1HCHO	0.43	
		$CH_3C(O)CH=CHC1H$-O-$C1(CH_3)CHO$	0.39	
		HCHO	0.38	
		$CH_3C(O)CH(OOH)CH(OH)C1H$-O-$C1(CH_3)CHO$	0.34	
		$CH_3C(O)OOH$	0.34	
		$HOC(O)C1H$-O-$C1(CH_3)CHO$	0.31	
		glyoxal	0.22	
		m-xylenol	0.22	
		$HOOC(O)CH=C(CH_3)CHO$	0.21	
		$CH_3C(O)CH=CHC(O)OOH$	0.20	
		$CH_3C(O)C(O)CH(OH)C1H$-O-$C1(CH_3)CHO$	0.18	
		TT801J	0.17	
		TT8004	0.16	
		CH_3O_2	0.15	
	$1x10^{12}$	CH_3OOH	0.48	56

		CO	0.19	
		HCHO	0.12	
isoprene	$1x10^{10}$	isoprene	3.68	93
		ISOPOOH	2.80	
		$HOOCH_2CH=C(CH_3)CHO$	0.23	
	$1x10^{11}$	ISOPOOH	0.37	36
		IEPOX	0.33	

References:

Back, R.A. and S. Yamamoto, "The gas-phase photochemistry and thermal decomposition of glyoxylic acid," Can. J. Chem. 63, 542-548, doi: 10.1021/j100250a014, 1985.

Bloss, C., Wagner, V., Jenkin, M. E., Volkamer, R., Bloss, W. J., Lee, J. D., Heard, D. E., Wirtz, K., Martin-Reviejo, M., Rea, G., Wenger, J. C. and Pilling, M. J.: Development of a detailed chemical mechanism (MCMv3.1) for the atmospheric oxidation of aromatic hydrocarbons, Atmos. Chem. Phys., 5(3), 641–664, doi:10.5194/acp-5-641-2005, 2005.

Cooper, G., J.E. Anderson, and C.E. Brion, "Absolute photoabsorption and photoionization of formaldehyde in the VUV and soft X-ray regions (3-200 eV)," Chem. Phys. 209, 61-77, doi: 10.1016/0301-0104(96)00079-1, 1996.

Dillon, T.J., A. Horowitz, D. Hölscher, J.N. Crowley, L. Vereecken, and J. Peeters, "Reaction of HO with hydroxyacetone ($HOCH_2C(O)CH_3$): rate coefficients (233-363 K) and mechanism," Phys. Chem. Chem. Phys. 8, 236-246, doi: 10.1039/B513056E, 2006.

Gierczak, T., M.K. Gilles, S. Bauerle, and A.R. Ravishankara, "Reaction of hydroxyl radical with acetone. 1. Kinetics of the reactions of OH, OD, and ^{18}OH with acetone and acetone-d_6," J. Phys. Chem. A 107, 5014-5020, doi: 10.1021/jp027301a, 2003.

Jenkin, M. E., Young, J. C. and Rickard, A. R.: The MCM v3.3.1 degradation scheme for isoprene, Atmos. Chem. Phys., 15(20), 11433–11459, doi:10.5194/acp-15-11433-2015, 2015.

Karunanandan, R., D. Hölscher, T.J. Dillon, A. Horowitz, and J.N. Crowley, Reaction of HO with glycolaldehyde, HOCH2CHO: Rate coefficients (240-362 K) and mechanism, J. Phys.Chem. A 111, 897-908, doi: 10.1021/jp0649504, 2007.

Keller-Rudek, H., Moortgat, G. K., Sander, R., and Sörensen, R.The MPI-Mainz UV/VIS spectral atlas of gaseous molecules of atmospheric interest, Earth Syst. Sci. Data, 5, 365–373, doi:10.5194/essd-5-365-2013, 2013.

Lee, A.M.D., J.D. Coe, S. Ullrich, M.L. Ho, S.-J. Lee, B.-M. Cheng, M.Z. Zgierski, I-C. Chen, T.J. Martinez, and A. Stolow, Substituent effects on dynamics at conical intersections: α,β-enones, J. Phys. Chem. A 111, 11948-11960, doi: 10.1021/jp074622j, 2007.

Lucazeau, G., and C. Sandorfy, On the far-ultraviolet spectra of some simple aldehydes, J. Mol. Spectrosc. 35, 214-231, doi: 10.1016/0022-2852(70)90199-2, 1970.

Moortgat, G., Wirtz, K., Pons, N., Jensen, N., Horth, J., Winterhalter, R., Ruppert, L., Magneron, L., Tadic, J., and Mellouki,A.: Trends in tropospheric photodissociation rates of selected carbonyl compounds, in: Proceedings of the EC/Eurotrac-2 joint workshop, edited by: Vogt, R. and Axelsdottir, G., 28–31, ISBN 3-00-005414-6, Aachen, 1999.

Orlando, J.J., G.S. Tyndall, J.-M. Fracheboud, E.G. Estupiñan, S. Haberkorn, and A. Zimmer, The rate and mechanism of the gas-phase oxidation of hydroxyacetone, Atmos. Environ. 33, 1621-1629, doi: 10.1016/S1352-2310(98)00386-0, 1999.

Röth, E.-P. and D.H. Ehhalt, A simple formulation of the CH_2O photolysis quantum yields, Atmos. Chem. Phys., 15, 7195-7202, doi:10.5194/acp-15-7195-2015, doi:10.5194/acp-15-7195-2015, 2015.

Sander, S. P., J. Abbatt, J. R. Barker, J. B. Burkholder, R. R. Friedl, D. M. Golden, R. E. Huie, C. E. Kolb, M. J. Kurylo, G.K. Moortgat, V. L. Orkin and P. H. Wine, "Chemical Kinetics and Photochemical Data for Use in Atmospheric Studies, Evaluation No. 17," JPL Publication 10-6, Jet Propulsion Laboratory, Pasadena (2011). http://jpldataeval.jpl.nasa.gov.

Volkamer, R., P. Spietz, J.P. Burrows, and U. Platt, High-resolution absorption cross-sections of glyoxal in the UV-vis and IR spectral ranges, J. Photochem. Photobiol. A: Chem. 172, 35-46, doi: 10.1016/j.jphotochem.2004.11.011, 2005.

Yamamoto, S., and R.A. Back, R.A., The gas-phase photochemistry of oxalic acid, J. Phys. Chem., 89,(4) 622-625, doi:10.1021/j100250a014, 1985.

Zhu, L., D. Kellis, and C.-F. Ding, "Photolysis of glyoxal at 193, 248, 308, and 351 nm," Chem. Phys. Lett. 257, 487-491.